Poisson-Randomized Gamma Dynamical Systems

Aaron Schein
Data Science Institute
Columbia University

Scott W. Linderman
Department of Statistics
Stanford University

Mingyuan Zhou
McCombs School of Business
University of Texas at Austin

David M. Blei
Department of Statistics
Columbia University

Hanna Wallach
Microsoft Research
New York, NY

Abstract

This paper presents the Poisson-randomized gamma dynamical system (PRGDS), a model for sequentially observed count tensors that encodes a strong inductive bias toward sparsity and burstiness. The PRGDS is based on a new motif in Bayesian latent variable modeling, an alternating chain of discrete Poisson and continuous gamma latent states that is analytically convenient and computationally tractable. This motif yields closed-form complete conditionals for all variables by way of the Bessel distribution and a novel discrete distribution that we call the shifted confluent hypergeometric distribution. We draw connections to closely related models and compare the PRGDS to these models in studies of real-world count data sets of text, international events, and neural spike trains. We find that a sparse variant of the PRGDS, which allows the continuous gamma latent states to take values of exactly zero, often obtains better predictive performance than other models and is uniquely capable of inferring latent structures that are highly localized in time.

1 Introduction

Political scientists routinely analyze event counts of the number of times country i took action a toward country j during time step t [1]. Such data can be represented as a sequence of count tensors $\boldsymbol{Y}^{(1)}, \ldots, \boldsymbol{Y}^{(T)}$ each of which contains the $V \times V \times A$ event counts for that time step for every combination of V sender countries, V receivers, and A action types. International event data sets exhibit "complex dependence structures" [2] like coalitions of countries and bursty temporal dynamics. These dependence structures violate the independence assumptions of the regression-based methods that political scientists have traditionally used to test theories of international relations [3–5]. Political scientists have therefore advocated for using latent variable models to infer unobserved structures as a way of controlling for them [6]. This approach motivates interpretable yet expressive models that are capable of capturing a variety of complex dependence structures. Recent work has applied tensor factorization methods to international event data sets [7–11] to infer coalition structures among countries and topic structures among actions; however, these methods assume that the sequentially observed count tensors are exchangeable, thereby failing to capture the bursty temporal dynamics inherent to such data sets.

Sequentially observed count tensors present unique statistical challenges because they tend to be bursty [12], high-dimensional, and sparse [13, 14]. There are few models that are tailored to the challenging properties of both time series and count tensors. In recent years, Poisson factorization has emerged as a framework for modeling count matrices [15–20] and tensors [13, 21, 9]. Although factorization methods generally scale with the size of the matrix or tensor, many Poisson factorization models yield inference algorithms that scale linearly with the number of non-zero entries. This property allows researchers to efficiently infer latent structures from massive tensors, provided these tensors are sparse; however, this property is unique to a subset of Poisson factorization models that only posit

(a) Poisson–gamma dynamical systems [22] (b) Poisson-randomized gamma dynamical systems
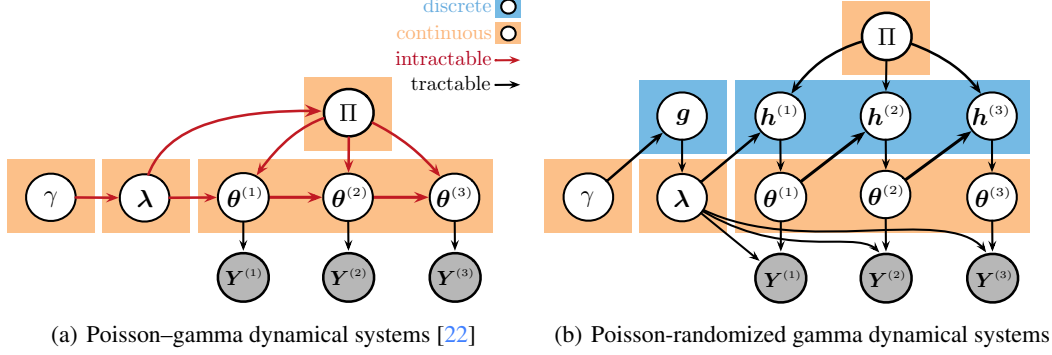
Figure 1: *Left*: The PGDS imposes dependencies directly between the gamma latent states, preventing closed-form complete conditionals. *Right*: The PRGDS (this paper) breaks these dependencies with discrete Poisson latent states—doing so yields closed-form conditionals for all variables without data augmentation.

non-negative prior distributions, which are difficult to chain in state-space models for time series. Hierarchical compositions of non-negative priors—notably, gamma and Dirichlet distributions—typically introduce non-conjugate dependencies that require innovative approaches to posterior inference.

This paper fills a gap in the literature between Poisson factorization models that are tractable—i.e., yielding closed-form complete conditionals that make inference algorithms easy to derive—and those that are expressive—i.e., capable of capturing a variety of complex dependence structures. To do so, we introduce an alternating chain of discrete Poisson and continuous gamma latent states, a new modeling motif that is analytically convenient and computationally tractable. We rely on this motif to construct the Poisson-randomized gamma dynamical system (PRGDS), a model for sequentially observed count tensors that is tractable, expressive, and efficient. The PRGDS is closely related to the Poisson–gamma dynamical system (PGDS) [22], a recently introduced model for dynamic count matrices, that is based on non-conjugate chains of gamma states. These chains are intractable; thus, posterior inference in the PGDS relies on sophisticated data augmentation schemes that are cumbersome to derive and impose unnatural restrictions on the priors over other variables. In contrast, the PRGDS introduces intermediate Poisson states that break the intractable dependencies between the gamma states (see Fig. 1). Although this motif is only semi-conjugate, it is tractable, yielding closed-form complete conditionals for the Poisson states by way of the little-known Bessel distribution [23] and a novel discrete distribution that we derive and call the *shifted confluent hypergeometric (SCH) distribution*.

We study the inductive bias of the PRGDS by comparing its smoothing and forecasting performance to that of the PGDS and two other baselines on a range of real-world count data sets of text, international events, and neural spike data. For smoothing, we find that the PRGDS performs better than or similarly to the PGDS; for forecasting, we find the converse relationship. Both models outperform the other baselines. Using a specific hyperparameter setting, the PRGDS permits the continuous gamma latent states to take values of exactly zero, thereby encoding a unique inductive bias tailored to sparsity and burstiness. We find that this sparse variant always obtains better smoothing and forecasting performance than the non-sparse variant. We also find that this sparse variant yields a qualitatively broader range of latent structures—specifically, bursty latent structures that are highly localized in time.

2   Poisson-randomized gamma dynamical systems (PRGDS)

Notation. Consider a data set of sequentially observed count tensors $\boldsymbol{Y}^{(1)}, \dots, \boldsymbol{Y}^{(T)}$, each of which has M modes. An entry $y_{\mathbf{i}}^{(t)} \in \{0, 1, 2, \dots\}$ in the tth tensor is subscripted by a multi-index $\mathbf{i} \equiv (\mathbf{i}_1, \dots, \mathbf{i}_M)$ that indexes into the M modes of the tensor. As an example, the event count of the number of times country i took action a toward country j during time step t can be written as $y_{\mathbf{i}}^{(t)}$ where the multi-index corresponds to the sender, receiver, and action type—i.e., $\mathbf{i} = (i, j, a)$.

Generative process. The PRGDS is a form of canonical polyadic decomposition [24] that assumes

$$y_{\mathbf{i}}^{(t)} \sim \text{Pois}\Big(\rho^{(t)} \sum_{k=1}^{K} \lambda_k \, \theta_k^{(t)} \prod_{m=1}^{M} \phi_{k\mathbf{i}_m}^{(m)} \Big), \tag{1}$$

2

where $\theta_k^{(t)}$ represents the activation of the kth component at time step t. Each component represents a dependence structure in the data set by way of a factor vector $\boldsymbol{\phi}_k^{(m)}$ for each mode m. For international events, the first factor vector $\boldsymbol{\phi}_k^{(1)} = (\phi_{k1}^{(1)}, \ldots, \phi_{kV}^{(1)})$ represents the rate at which each of the V countries acts as a sender in the kth component while the second factor vector $\boldsymbol{\phi}_k^{(2)}$ represents the rate at which each country acts as a receiver. The weights λ_k and $\rho^{(t)}$ represent the scales of component k and time step t. The PRGDS is stationary if $\rho^{(t)} = \rho$. We posit the following conjugate priors:

$$\rho^{(t)} \sim \text{Gam}(a_0, b_0) \quad \text{and} \quad \boldsymbol{\phi}_k^{(m)} \sim \text{Dir}(a_0, \ldots, a_0). \tag{2}$$

The PRGDS is characterized by an alternating chain of discrete and continuous latent states. The continuous states $\theta_k^{(1)}, \ldots, \theta_k^{(T)}$ evolve via the intermediate discrete states $h_k^{(1)}, \ldots, h_k^{(T)}$ as follows:

$$\theta_k^{(t)} \sim \text{Gam}\left(\epsilon_0^{(\theta)} + h_k^{(t)}, \tau\right) \quad \text{and} \quad h_k^{(t)} \sim \text{Pois}\left(\tau \sum_{k_2=1}^{K} \pi_{kk_2} \theta_{k_2}^{(t-1)}\right), \tag{3}$$

where we define $\theta_k^{(0)} = \lambda_k$ to be the per-component weight from Eq. (1). In other words, the PRGDS assumes that $\theta_k^{(t)}$ is conditionally gamma distributed with rate τ and shape equal to $h_k^{(t)}$ plus hyperparameter $\epsilon_0^{(\theta)} \geq 0$. We adopt the convention that a gamma random variable will be zero, almost surely, if its shape is zero. Therefore, setting $\epsilon_0^{(\theta)} = 0$ defines a sparse variant of the PRGDS, where the gamma latent state $\theta_k^{(t)}$ takes the value of exactly zero provided $h_k^{(t)} = 0$—i.e., $\theta_k^{(t)} \overset{\text{a.s.}}{=} 0$ if $h_k^{(t)} = 0$.

The *transition weight* π_{kk_2} in Eq. (3) represents how strongly component k_2 excites component k at the next time step. We view these weights collectively as a $K \times K$ transition matrix Π and impose Dirichlet priors over the columns of this matrix. We also place a gamma prior over concentration parameter τ. This prior is conjugate to the gamma and Poisson distributions in which it appears:

$$\tau \sim \text{Gam}(\alpha_0, \alpha_0) \quad \text{and} \quad \boldsymbol{\pi}_k \sim \text{Dir}(a_0, \ldots, a_0) \quad \text{such that} \quad \sum_{k_1}^{K} \pi_{k_1 k} = 1. \tag{4}$$

For the per-component weights $\lambda_1, \ldots, \lambda_K$, we use a hierarchical prior with a similar flavor to Eq. (3):

$$\lambda_k \sim \text{Gam}\left(\frac{\epsilon_0^{(\lambda)}}{K} + g_k, \beta\right) \quad \text{and} \quad g_k \sim \text{Pois}\left(\frac{\gamma}{K}\right), \tag{5}$$

where $\epsilon_0^{(\lambda)}$ is analogous to $\epsilon_0^{(\theta)}$. Finally, we use the following gamma priors, which are both conjugate:

$$\gamma \sim \text{Gam}(a_0, b_0) \quad \text{and} \quad \beta \sim \text{Gam}(\alpha_0, \alpha_0). \tag{6}$$

The PRGDS has five fixed hyperparameters: $\epsilon_0^{(\theta)}$, $\epsilon_0^{(\lambda)}$, α_0, a_0, and b_0. For the empirical studies in § 5, we set $a_0 = b_0 = 0.01$ to define weakly informative gamma and Dirichlet priors and set $\alpha_0 = 10$ to define a gamma prior that promotes values close to 1; we consider $\epsilon_0^{(\theta)} \in \{0, 1\}$ and set $\epsilon_0^{(\lambda)} = 1$.

Properties. In Eq. (5), both $\epsilon_0^{(\lambda)}$ and γ are divided by the number of components K. This means that as the number of components grows $K \to \infty$, the expected sum of the weights remains finite and fixed:

$$\sum_{k=1}^{\infty} \mathbb{E}[\lambda_k] = \sum_{k=1}^{\infty} \left(\frac{\epsilon_0^{(\lambda)}}{K} + \mathbb{E}[g_k]\right)\beta^{-1} = \sum_{k=1}^{\infty} \left(\frac{\epsilon_0^{(\lambda)}}{K} + \frac{\gamma}{K}\right)\beta^{-1} = \left(\epsilon_0^{(\lambda)} + \gamma\right)\beta^{-1}. \tag{7}$$

This prior encodes an inductive bias toward small values of λ_k and may be interpreted as the finite truncation of a novel Bayesian nonparametric process. A small value of λ_k shrinks the Poisson rates of both $y_{\mathbf{i}}^{(t)}$ and the first discrete latent state $h_k^{(0)}$. As a result, this prior encourages the PRGDS to only infer components that are both predictive of the data and useful for capturing the temporal dynamics.

The marginal expectation of $\boldsymbol{\theta}^{(t)} = (\theta_1^{(t)}, \ldots, \theta_K^{(t)})$ takes the form of a linear dynamical system:

$$\mathbb{E}\left[\boldsymbol{\theta}^{(t)} \mid \boldsymbol{\theta}^{(t-1)}\right] = \mathbb{E}\left[\mathbb{E}\left[\boldsymbol{\theta}^{(t)} \mid \boldsymbol{h}^{(t-1)}\right]\right] = \epsilon_0^{(\theta)} \tau^{-1} + \Pi \boldsymbol{\theta}^{(t-1)}. \tag{8}$$

This is because $\mathbb{E}\left[\theta_k^{(t)}\right] = \left(\epsilon_0^{(\theta)} + \mathbb{E}\left[h_k^{(t)}\right]\right)\tau^{-1} = \left(\epsilon_0^{(\theta)} + \tau \sum_{k_2=1}^{K} \pi_{kk_2} \theta_{k_2}^{(t)}\right)\tau^{-1}$ by iterated expectation. Concentration parameter τ appears in both the Poisson and gamma distributions in Eq. (3). It contributes to the variance of the PRGDS, while simultaneously canceling out of the expectation in Eq. (8), except for its role in the additive term $\epsilon_0^{(\theta)} \tau^{-1}$, which itself disappears when $\epsilon_0^{(\theta)} = 0$.

Finally, we can analytically marginalize out all of the discrete Poisson latent states to obtain a purely continuous dynamical system. When $\epsilon_0^{(\theta)} > 0$, this dynamical system can be written as follows:

$$\theta_k^{(t)} \sim \text{RG1}\left(\epsilon_0^{(\theta)}, \tau \sum_{k_2=1}^{K} \pi_{kk_2} \theta_{k_2}^{(t-1)}, \tau\right), \tag{9}$$

where RG1 denotes the randomized gamma distribution of the first type [23, 25]. When $\epsilon_0^{(\theta)} = 0$, the dynamical system can be written in terms of a limiting form of the RG1. We describe the RG1 in Fig. 2.
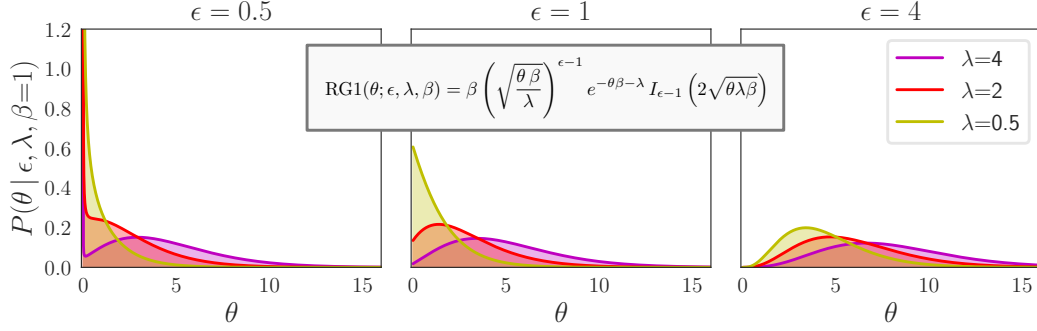
3

Figure 2: The randomized gamma distribution of the first type (RG1) [23, 25] has support $\theta > 0$ and is defined by three parameters: $\epsilon, \lambda, \beta > 0$. Its PDF is displayed in the figure; $I_{\epsilon-1}(\cdot)$ is the modified Bessel function of the first kind [26]. When $\epsilon < 1$ (*left*), the RG1 resembles a soft "spike-and-slab" distribution; when $\epsilon \geq 1$ (*middle and right*), it resembles a more-dispersed form of the gamma distribution. The Poisson-randomized gamma distribution [27], which includes zeros in its support (i.e., $\theta \geq 0$), is a limiting case of the RG1 that occurs when $\epsilon \to 0$.

3 Related work

The PRGDS is closely related to the Poisson–gamma dynamical system (PGDS) [22]. In the PGDS,

$$\theta_k^{(t)} \sim \text{Gam}\Big(\tau \sum_{k_2=1}^{K} \pi_{kk_2} \theta_{k_2}^{(t-1)}, \tau\Big) \text{ such that } \mathbb{E}\big[\boldsymbol{\theta}^{(t)} \mid \boldsymbol{\theta}^{(t-1)}\big] = \Pi\,\boldsymbol{\theta}^{(t-1)}. \tag{10}$$

The PGDS imposes non-conjugate dependencies directly between the gamma latent states. The complete conditional $P(\theta_k^{(t)}|-)$ is not available in closed form, and posterior inference relies on a sophisticated data augmentation scheme. The PRGDS instead introduces intermediate Poisson states that break the intractable dependencies between the gamma states; we visualize this in Fig. 1. Although the Poisson distribution is not a conjugate prior for the gamma rate, this motif is still tractable, yielding the complete conditional $P(h_k^{(t)}|-)$ in closed form, as we explain in § 4. The PGDS is limited by the data augmentation scheme that it relies on for posterior inference—specifically, this augmentation scheme does not allow λ_k to appear in the Poisson rate of $y_{\mathbf{i}}^{(t)}$ in Eq. (1). To encourage parsimony, the PGDS instead draws $\lambda_k \sim \text{Gam}(\frac{\gamma}{K}, \beta)$ and then uses these per-component weights to shrink the transition matrix Π. This approach introduces additional intractable dependencies that require a different data augmentation scheme for posterior inference. Finally, the data augmentation schemes additionally require that each factor vector $\boldsymbol{\phi}_k^{(m)}$ and each column $\boldsymbol{\pi}_k$ of the transition matrix are Dirichlet distributed. We note that although we also use Dirichlet distributions in this paper, this is a choice rather than a requirement imposed by the PRGDS.

The PGDS and its "deep" variants [28, 29] generalize gamma process dynamic Poisson factor analysis (GP-DPFA) [30], which assumes a simple random walk $\theta_k^{(t)} \sim \text{Gam}\big(\theta_k^{(t-1)}, c^{(t)}\big)$; the model of Yang and Koeppl is also closely related [31]. These models belong to a line of work exploring the "augment-and-conquer" data augmentation scheme [32] for posterior inference in hierarchies of gamma variables chained via their shapes and linked to Poisson observations. Beyond models for time series, this motif can be used to build belief networks [33]. An alternative approach is to chain gamma variables via their rates—e.g., $\theta^{(t)} \sim \text{Gam}\big(a, \theta^{(t-1)}\big)$. This motif is conjugate and tractable, and has been applied to models for time series [34–36] and deep belief networks [37]. However, unlike the shape, the rate contributes to the variance of the gamma quadratically. Rate chains can therefore be highly volatile.

More broadly, gamma shape and rate chains are examples of non-negative chains. Such chains are especially well motivated in the context of Poisson factorization, which is particularly efficient when only non-negative prior distributions are used. In general, Poisson factorization assumes that each observed count $y_{\mathbf{i}}$ is drawn from a Poisson distribution with a latent rate $\mu_{\mathbf{i}}$ that is some function of the model parameters—i.e., $y_{\mathbf{i}} \sim \text{Pois}(\mu_{\mathbf{i}})$. When the rate is linear—i.e., $\mu_{\mathbf{i}} = \sum_{k=1}^{K} \mu_{\mathbf{i}k}$—Poisson factorization is allocative [38] and admits a latent source representation [16, 18], where $y_{\mathbf{i}} \triangleq \sum_{k=1}^{K} y_{\mathbf{i}k}$ is defined to be the sum of K latent sources $y_{\mathbf{i}1}, \dots, y_{\mathbf{i}K}$ and $y_{\mathbf{i}k} \sim \text{Pois}(\mu_{\mathbf{i}k})$. Conditioning on the latent sources often induces conditional independencies that, in turn, facilitate closed-form, efficient, and parallelizable posterior inference. The first step in either MCMC or variational inference

is therefore to update each latent source from its complete conditional, which is multinomial [39]:

$$\left((y_{\mathbf{i}1}, \ldots, y_{\mathbf{i}K}) \mid - \right) \sim \text{Multinom}\left(y_{\mathbf{i}}, (\mu_{\mathbf{i}1}, \ldots, \mu_{\mathbf{i}K})\right), \tag{11}$$

where the normalization of the non-negative rates $\mu_{\mathbf{i}1}, \ldots, \mu_{\mathbf{i}K}$ into a probability vector is left implicit. When the observed count is zero—i.e., $y_{\mathbf{i}} = 0$—the sources are also zero—i.e., $y_{\mathbf{i}k} \stackrel{\text{a.s.}}{=} 0$—and no computation is required to update them. As a result, any Poisson factorization model that admits a latent source representation scales linearly with only the non-zero entries. This property is indispensable when modeling count tensors which typically contain exponentially more zeros than non-zeros [40]. We emphasize that although the PRGDS and PGDS are substantively different models, they are both instances of allocative Poisson factorization, so the time complexity of posterior inference for both models is the same and equal to $\mathcal{O}(SK)$ where S is the number of non-zero entries.

Because a latent source representation is only available when the rate $\mu_{\mathbf{i}}$ is a linear function of the model parameters and, by definition of the Poisson distribution, the rate must be non-negative, efficient Poisson factorization is only possible with non-negative priors. Modeling time series and other complex dependence structures via efficient Poisson factorization therefore requires developing novel motifs that exclude the Gaussian priors that researchers have traditionally relied on for analytic convenience and tractability. For example, the Poisson linear dynamical system [41–43] links the widely used Gaussian linear dynamical system [44, 45] to Poisson observations via an exponential link function—i.e., $\mu_{\mathbf{i}} = \exp\left(\sum_k \cdots\right)$. This approach, which is based on the generalized linear model [46], relies on a non-linear link function and therefore does not admit a latent source representation. Another approach is to use log-normal priors, as in dynamic Poisson factorization [47]; however, the log-normal is not conjugate to the Poisson distribution and does not yield closed-form conditionals.

There is also a long tradition of autoregressive models for time series of counts, including variational autoregressive models [48] and models that are based on the Hawkes process [49–52]. This approach avoids the challenge of constructing tractable state-space models from non-negative priors by modeling temporal correlations directly between the observed counts. However, for high-dimensional data, such as sequentially observed count tensors, an autoregressive approach is often impractical.

4 Posterior inference

Iteratively re-sampling each latent variable in the PRGDS from its complete conditional constitutes a Gibbs sampling algorithm. The complete conditionals for all variables are immediately available in closed form without data augmentation. We provide conditionals for the variables with non-standard priors below; the remaining conditionals are in the supplementary material. The PRGDS is based on a new motif in Bayesian latent variable modeling. We introduce the motif in its general form, derive its conditionals, and then use these to obtain the closed-form complete conditionals for the PRGDS.

4.1 Poisson–gamma–Poisson chains

Consider the following model of count m involving variables θ and h and fixed $c_1, c_2, c_3, \epsilon_0^{(\theta)} > 0$:

$$m \sim \text{Pois}\left(\theta c_3\right), \ \ \theta \sim \text{Gam}\left(\epsilon_0^{(\theta)} + h, c_2\right), \ \text{and} \ h \sim \text{Pois}\left(c_1\right). \tag{12}$$

This model is semi-conjugate. The gamma prior over θ is conjugate to the Poisson and its posterior is

$$\left(\theta \mid - \right) \sim \text{Gam}\left(\epsilon_0^{(\theta)} + h + m, \ c_2 + c_3\right). \tag{13}$$

The Poisson prior over h is not conjugate to the gamma; however, despite this, the posterior of h is still available in closed form by way of the Bessel distribution [23], which we define in Fig. 3(a):

$$\left(h \mid - \right) \sim \text{Bes}\left(\epsilon_0^{(\theta)} - 1, \ 2\sqrt{\theta c_2 c_1}\right). \tag{14}$$

The Bessel distribution can be sampled efficiently [53]; our Cython implementation is available online.[1] Provided that $\epsilon_0^{(\theta)} > 0$, sampling θ and h iteratively from Eqs. (13) and (14) constitutes a valid Markov chain for posterior inference. When $\epsilon_0^{(\theta)} = 0$, though, $\theta \stackrel{\text{a.s.}}{=} 0$ if $h = 0$, and vice versa. As a result, this Markov chain has an absorbing condition at $h = 0$ and violates detailed balance. In this case, we must therefore sample h with θ marginalized out. Toward that end, we prove Theorem 1.

---

[1] https://github.com/aschein/PRGDS

(a) Bessel distribution [23]   (b) Shifted confluent hypergeometric (SCH) distribution
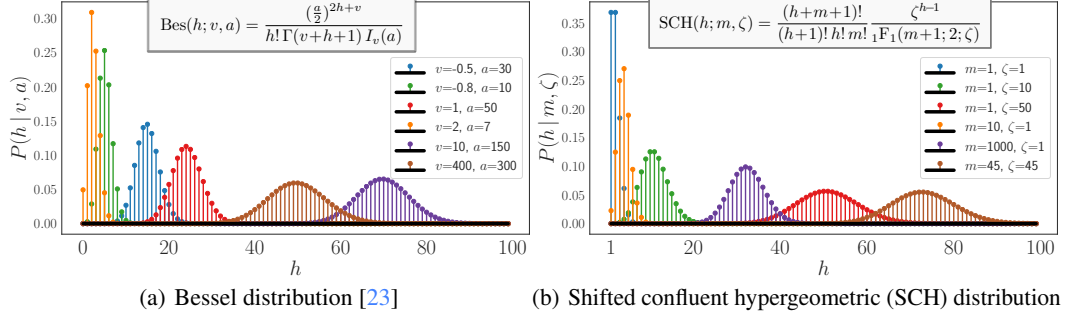
Figure 3: Two discrete distributions that arise as posteriors in Poisson–gamma–Poisson chains.

Theorem 1: *The incomplete conditional $P(h \mid \epsilon_0^{(\theta)} = 0, -\backslash\theta) \triangleq \int P(h, \theta \mid \epsilon_0^{(\theta)} = 0, -) \, \mathrm{d}\theta$ is*

$$(h \mid -\backslash\theta) \sim \begin{cases} \mathrm{Pois}\left(\frac{c_1 c_2}{c_3 + c_2}\right) & \text{if } m = 0 \\ \mathrm{SCH}\left(m, \frac{c_1 c_2}{c_3 + c_2}\right) & \text{otherwise,} \end{cases} \tag{15}$$

where SCH denotes the shifted confluent hypergeometric distribution. We describe the SCH in Fig. 3(b) and provide further information in the supplementary material, including the derivation of its PMF, PGF, and mode, along with details of how we sample from it and the proof for Theorem 1.

4.2 Closed-form complete conditionals for the PRGDS

The PRGDS admits a latent source representation, so the first step of posterior inference is therefore

$$\left((y_{\mathbf{i}k}^{(t)})_{k=1}^K \mid -\right) \sim \mathrm{Multinom}\left(y_{\mathbf{i}}^{(t)}, \left(\lambda_k \, \theta_k^{(t)} \prod_{m=1}^M \phi_{k i_m}^{(m)}\right)_{k=1}^K\right). \tag{16}$$

We may similarly represent $h_k^{(t)}$ under its latent source representation—i.e., $h_k^{(t)} \equiv h_{k\cdot}^{(t)} = \sum_{k_2=1}^K h_{k k_2}^{(t)}$, where $h_{k k_2}^{(t)} \sim \mathrm{Pois}\left(\tau \, \pi_{k k_2} \theta_{k_2}^{(t-1)}\right)$. When notationally convenient, we use dot-notation ("·") to denote summing over a mode. In this case, $h_{k\cdot}^{(t)}$ denotes the sum of the kth row of the $K \times K$ matrix of latent counts $h_{k k_2}^{(t)}$. The complete conditional of the kth row of counts, when conditioned on their sum $h_{k\cdot}^{(t)}$, is

$$\left((h_{k k_2}^{(t)})_{k_2=1}^K \mid -\right) \sim \mathrm{Multinom}\left(h_{k\cdot}^{(t)}, \, (\pi_{k k_2} \theta_{k_2}^{(t-1)})_{k_2=1}^K\right). \tag{17}$$

To derive the conditional for $\theta_k^{(t)}$ we aggregate the Poisson variables that depend on it. By Poisson additivity, the column sum $h_{\cdot k}^{(t+1)} = \sum_{k_1=1}^K h_{k_1 k}^{(t+1)}$ is distributed as $h_{\cdot k}^{(t+1)} \sim \mathrm{Pois}\left(\theta_k^{(t)} \, \tau \, \pi_{\cdot k}\right)$ and similarly $y_{\cdot k}^{(t)}$ is distributed as $y_{\cdot k}^{(t)} \sim \mathrm{Pois}\left(\theta_k^{(t)} \rho^{(t)} \lambda_k \prod_{m=1}^M \phi_{k\cdot}^{(m)}\right)$. The count $m_k^{(t)} \triangleq h_{\cdot k}^{(t+1)} + y_{\cdot k}^{(t)}$ isolates all dependence on $\theta_k^{(t)}$ and is also Poisson distributed. By gamma–Poisson conjugacy, the conditional of $\theta_k^{(t)}$ is

$$\left(\theta_k^{(t)} \mid -\right) \sim \mathrm{Gam}\left(\epsilon_0^{(\theta)} + h_{k\cdot}^{(t)} + m_k^{(t)}, \, \tau + \tau \, \pi_{\cdot k} + \rho^{(t)} \lambda_k \prod_{m=1}^M \phi_{k\cdot}^{(m)}\right). \tag{18}$$

When $\epsilon_0^{(\theta)} > 0$, we apply the identity in Eq. (14) and sample $h_{k\cdot}^{(t)}$ from its complete conditional:

$$\left(h_{k\cdot}^{(t)} \mid -\right) \sim \mathrm{Bessel}\left(\epsilon_0^{(\theta)} - 1, \, 2\sqrt{\theta_k^{(t)} \tau^2 \sum_{k_2=1}^K \pi_{k k_2} \theta_{k_2}^{(t-1)}}\right). \tag{19}$$

When $\epsilon_0^{(\theta)} = 0$, we instead apply Theorem 1 to sample $h_{k\cdot}^{(t)}$, where $m_k^{(t)}$ is analogous to m in Eq. (15):

$$\left(h_{k\cdot}^{(t)} \mid -\backslash\theta_k^{(t)}\right) \sim \begin{cases} \mathrm{Pois}(\zeta_k^{(t)}) & \text{if } m_k^{(t)} = 0 \\ \mathrm{SCH}(m_k^{(t)}, \, \zeta_k^{(t)}) & \text{otherwise} \end{cases} \quad \text{where} \quad \zeta_k^{(t)} \triangleq \frac{\tau^2 \sum_{k_2=1}^K \pi_{k k_2} \theta_{k_2}^{(t-1)}}{\tau + \tau \, \pi_{\cdot k} + \rho^{(t)} \lambda_k \prod_{m=1}^M \phi_{k\cdot}^{(m)}}. \tag{20}$$

The complete conditionals for λ_k and g_k follow from applying the same Poisson–gamma–Poisson identities, while the complete conditionals for γ, β, $\phi_k^{(m)}$, π_k, and τ all follow from conjugacy.

(a) Matrix empirical studies (originally described by Schein et al. [22])   (b) Tensor empirical studies
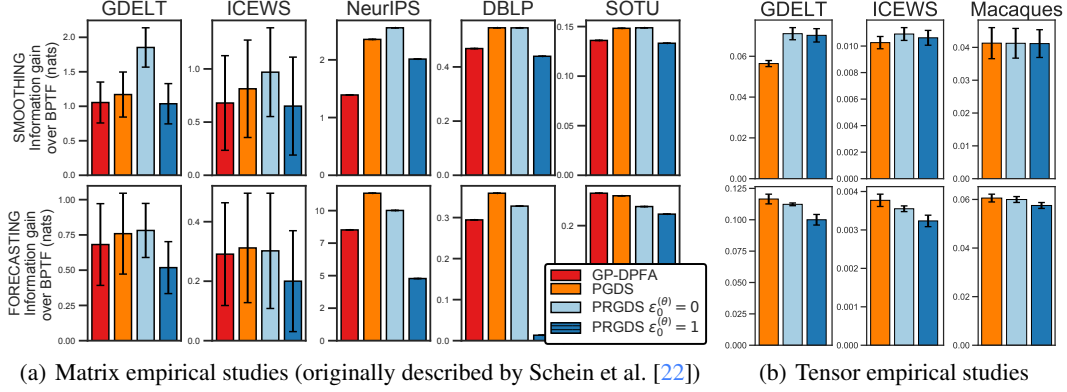
Figure 4: The smoothing performance (top row) or forecasting performance (bottom row) of each model is quantified by its information gain over a non-dynamic baseline (BPTF [9]), where higher values are better.

5 Empirical studies

As explained in the previous section, the Poisson–gamma–Poisson motif of the PRGDS (see § 4.1) yields a more tractable (see Fig. 1) and flexible (see § 3) model than previous models. This motif also encodes a unique inductive bias tailored to sparsity and burstiness that we test by comparing the PRGDS to the PGDS (described in § 3). As we can see by comparing Eqs. (9) and (10), comparing these models isolates the impact of the Poisson–gamma–Poisson motif. Because the PGDS was previously introduced to model a $T \times V$ matrix Y of sequentially observed V-dimensional count vectors $\boldsymbol{y}^{(1)}, \ldots, \boldsymbol{y}^{(T)}$, we generalize the PGDS to M-mode tensors and provide derivations of its complete conditionals in the supplementary material. Our Cython implementation of this generalized PGDS (and the PRGDS) is available online. We also compare the variant of the PRGDS with $\epsilon_0^{(\theta)} = 1$ to the variant with $\epsilon_0^{(\theta)} = 0$, which allows the continuous gamma latent states to take values of exactly zero.

Setup. Our empirical studies all have the following setup. For each data set $\boldsymbol{Y}^{(1)}, \ldots, \boldsymbol{Y}^{(T)}$, the counts $\boldsymbol{Y}^{(t)}$ in randomly selected time steps are held out. Additionally, the counts in the last two time steps are always held out. Each model is fit to the data set using independent MCMC chains that impute the heldout counts and, ultimately, return a set of posterior samples of the latent variables. We distinguish the task of predicting the counts in intermediate time steps, known as smoothing, from the task of predicting the counts in the last two time steps, known as forecasting. To quantify the performance of each model, we use the S posterior samples returned by the independent chains to approximate the information rate [54] of the heldout counts—i.e.,
$R(\Delta) = -\frac{1}{|\Delta|} \sum_{(t,\mathbf{i}) \in \Delta} \log \left[\frac{1}{S} \sum_{s=1}^{S} \mathrm{Pois}\left(y_{\mathbf{i}}^{(t)}; \mu_{\mathbf{i},s}^{(t)} \right) \right]$, where Δ is the set of multi-indices of the heldout counts and $\mu_{\mathbf{i},s}^{(t)}$ is the expectation of heldout count $y_{\mathbf{i}}^{(t)}$ (defined in Eq. (1)) computed from the sth posterior sample. The information rate quantifies the average number of nats needed to compress each heldout count; it is equivalent to log perplexity [55] and to the negative of log pointwise predictive density (LPPD) [56]. In each study, we also fit Bayesian Poisson tensor factorization (BPTF) [9], a non-dynamic baseline that assumes that the count tensors at different time steps are i.i.d.—i.e., $y_{\mathbf{i}}^{(t)} \sim \mathrm{Pois}(\mu_{\mathbf{i}})$. For each model, we then report the information gain over BPTF, where higher values are better, which we compute by subtracting the information rate of the model from that of BPTF.

Matrices. We first replicated the empirical studies of Schein et al. [22]. These studies followed the setup described above and compared the PGDS to GP-DPFA [30], a simple dynamic baseline (described in § 3). The matrices in these studies were based on three text data sets—NeurIPS papers [57], DBLP abstracts [58], and State of the Union (SOTU) speeches [59]—where $y_v^{(t)}$ is the number of times word v occurs in time step t, and two international event data sets—GDELT [60] and ICEWS [61]—where $y_v^{(t)}$ is the number of times sender–receiver pair v interacted during time step t. We used the matrices and heldout time steps, along with the posterior samples for both PGDS and GP-DPFA, originally obtained by Schein et al. [22]. We then fit the PRGDS using the MCMC settings that they describe. In this matrix setting, BPTF reduces to $y_v^{(t)} \sim \mathrm{Pois}(\mu_v)$, where v indexes a single mode, and μ_v cannot be meaningfully factorized. We therefore posited a conjugate gamma prior over μ_v directly and drew exact posterior samples to compute the information rate. We depict the results in Fig. 4(a).

7
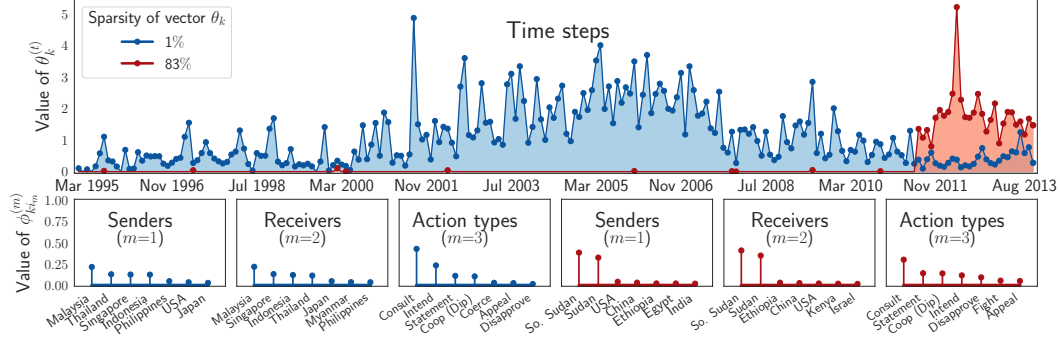
(a) We visualize two components inferred by a sparse variant of the PRGDS (i.e., $\epsilon_0^{(\theta)}=0$) from the ICEWS data set of international events. The blue component was also inferred by the other models while the red component was not. The red component is specific to South Sudan, as revealed by visualizing the largest values of the sender and receiver factor vectors (bottom row, red). South Sudan was not a country until July 2011 when it gained independence from Sudan. The gamma states (top row, red) are therefore sparse—i.e., $\theta_k^{(t)}=0$ in 94% of time steps (months) prior to July 2011 and in 83% of the time steps overall. In contrast, the blue component represents Southeast Asian relations, which are active in all time steps. The sparse variant can infer both temporally persistent latent structures (e.g., blue), as well as bursty latent structures that are highly localized in time (e.g., red).
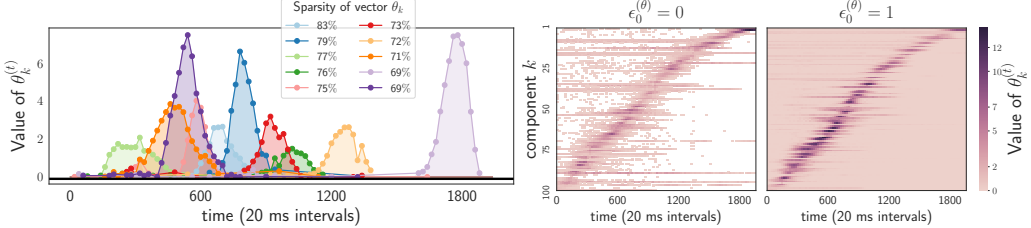
(b) We visualize components inferred by the PRGDS from the macaque motor cortex data set. The components inferred by a sparse variant (i.e., $\epsilon_0^{(\theta)}=0$) are bursty and highly localized in time (left), suggesting that neurons may be tuned to specific periods of the trial. The $K \times T$ gamma latent states for this variant of the PRGDS are sparse (middle, white cells correspond to $\theta_k^{(t)}=0$). The components (rows) are sorted by the time step in which the largest $\theta_k^{(t)}$ occurred, so the banded structure indicates that each component is only active for a short duration. In contrast, the components inferred by the non-sparse variant (i.e., $\epsilon_0^{(\theta)}=1$) are active in all time steps (right).

Figure 5: The PRGDS is capable of inferring latent structures that are highly localized in time.

Tensors. We used two international event data sets—GDELT and ICEWS—where $y_{i \xrightarrow{a} j}^{(t)}$ is the number of times country i took action a toward country j during time step t. Each data set consists of a sequence of count tensors, each of which contains the $V \times V \times A$ event counts for that time step, where $V = 249$ countries and $A = 20$ action types. For both data sets, we used months as time steps. For GDELT, we considered the date range 2003–2008, yielding $T = 72$; for ICEWS, we considered the date range 1995–2013, yielding $T = 228$. We also used a data set of multi-neuronal spike train recordings of macaque monkey motor cortexes [62, 63]. In this data set, a count $y_{ij}^{(t)}$ is the number of times neuron i spiked in trial j during time step t. These counts form a sequence of $N \times V$ matrices, where $N = 100$ is the number of neurons and $V = 1,716$ is the number of trials. We used 20-millisecond intervals as time steps, yielding $T = 162$. For each data set, we created three random masks, each corresponding to six heldout time steps in the range $[2, T-2]$. We fit each model to each data set and mask using two independent chains of 4,000 MCMC iterations, saving every 50th posterior sample after the first 1,000 iterations to compute the information rate. We also fit BPTF using variational inference as described by Schein et al. [9], and then sampled from the fitted variational posterior to compute the information rate. Following Schein et al. [22], we set $K = 100$ for all models. We depict the results in Fig. 4(b), where the error bars reflect variability across the random masks.

Quantitative results. In all sixteen studies, the dynamic models outperform BPTF. In all but one study, the PGDS and a sparse variant of the PRGDS (i.e., $\epsilon_0^{(\theta)}=0$) outperform the other models. For smoothing, the PRGDS performs better than or similarly to the PGDS. In five of the eight smoothing

8

studies, the sparse variant of the PRGDS obtains a higher information gain than the PGDS; in the remaining three smoothing studies, there is no discernible difference between the models. For forecasting, we find the converse relationship. In four of the eight forecasting studies, the PGDS obtains a higher information gain than the PGDS; in the remaining forecasting studies, there is no discernible difference. In all studies, the sparse variant of the PRGDS obtains better smoothing and forecasting performance than the non-sparse variant (i.e., $\epsilon_0^{(\theta)} = 1$). We conjecture that the better performance of the sparse variant can be explained by the form of the marginal expectation of $\boldsymbol{\theta}^{(t)}$ (see Eq. (8)). When $\epsilon_0^{(\theta)} > 0$ this expectation includes an additive term that grows as more time steps are forecast. When $\epsilon_0^{(\theta)} = 0$, this term disappears and the expectation matches that of the PGDS (see Eq. (10)).

Qualitative analysis. We also performed a qualitative comparison of the latent structures inferred by the different models and found that the sparse variant of the PRGDS inferred some components that the other models did not. Specifically, the sparse variant of the PRGDS is uniquely capable of inferring bursty latent structures that are highly localized in time; we visualize examples in Fig. 5. To compare the latent structures inferred by the PGDS and the PRGDS, we aligned the models' inferred components using the Hungarian bipartite matching algorithm [64] applied to the models' continuous gamma latent states. The kth component's activation vector $\boldsymbol{\theta}_k = (\theta_k^{(1)}, \ldots, \theta_k^{(T)})$ constitutes a signature of that component's activity; these signatures are sufficiently unique to facilitate alignment. In the supplementary material, we provide four components that are well aligned across the models. In Fig. 5(a), we visualize two components inferred by the sparse variant of the PRGDS; one of these components (blue) was also inferred by the other models, while the other component (red) was not.

6 Conclusion

We presented the Poisson-randomized gamma dynamical system (PRGDS), a tractable, expressive, and efficient model for sequentially observed count tensors. The PRGDS is based on a new modeling motif, an alternating chain of discrete Poisson and continuous gamma latent states that yields closed-form complete conditionals for all variables. We found that a sparse variant of the PRGDS, which allows the continuous gamma latent states to take values of exactly zero, often obtains better predictive performance than other models and infers latent structures that are highly localized in time.

References

[1] Philip A Schrodt. Event data in foreign policy analysis. *Foreign Policy Analysis: Continuity and Change in Its Second Generation*, 1995.

[2] Gary King. Proper nouns and methodological propriety: Pooling dyads in international relations data. *International Organization*, 55(2), 2001.

[3] Donald P Green, Soo Yeon Kim, and David H Yoon. Dirty pool. *International Organization*, 55(2), 2001.

[4] Paul Poast. (Mis)using dyadic data to analyze multilateral events. *Political Analysis*, 18(4), 2010.

[5] Robert S Erikson, Pablo M Pinto, and Kelly T Rader. Dyadic analysis in international relations: A cautionary tale. *Political Analysis*, 22(4), 2014.

[6] Brandon Stewart. Latent factor regressions for the social sciences. Technical report, Harvard University, 2014.

[7] Peter D Hoff and Michael D Ward. Modeling dependencies in international relations networks. *Political Analysis*, 12(2), 2004.

[8] Peter D Hoff. Multilinear tensor regression for longitudinal relational data. *Annals of Applied Statistics*, 9(3), 2015.

[9] Aaron Schein, John Paisley, David M Blei, and Hanna M Wallach. Bayesian Poisson tensor factorization for inferring multilateral relations from sparse dyadic event counts. In *ACM SIGKDD International Conference on Knowledge Discovery and Data Mining*, 2015.

[10] Peter D Hoff. Equivariant and scale-free Tucker decomposition models. *Bayesian Analysis*, 11 (3), 2016.

[11] Aaron Schein, Mingyuan Zhou, David M Blei, and Hanna M Wallach. Bayesian Poisson Tucker decomposition for learning the structure of international relations. In *International Conference on Machine Learning*, 2016.

[12] Jon Kleinberg. Bursty and hierarchical structure in streams. *Data Mining and Knowledge Discovery*, 7(4), 2003.

[13] Eric C Chi and Tamara G Kolda. On tensors, sparsity, and nonnegative factorizations. *SIAM Journal on Matrix Analysis and Applications*, 33(4), 2012.

[14] Tsuyoshi Kunihama and David B Dunson. Bayesian modeling of temporal dependence in large sparse contingency tables. *Journal of the American Statistical Association*, 108(504), 2013.

[15] John Canny. GaP: A factor model for discrete data. In *ACM SIGIR Conference on Research and Development in Information Retrieval*, 2004.

[16] David B Dunson and Amy H Herring. Bayesian latent variable models for mixed discrete outcomes. *Biostatistics*, 6(1), 2005.

[17] Michalis K Titsias. The infinite gamma–Poisson feature model. In *Advances in Neural Information Processing Systems*, 2008.

[18] A Taylan Cemgil. Bayesian inference for nonnegative matrix factorisation models. *Computational Intelligence and Neuroscience*, 2009.

[19] Mingyuan Zhou, Lauren Hannah, David B Dunson, and Lawrence Carin. Beta-negative binomial process and Poisson factor analysis. In *International Conference on Artificial Intelligence and Statistics*, 2012.

[20] Prem K Gopalan and David M Blei. Efficient discovery of overlapping communities in massive networks. *Proceedings of the National Academy of Sciences*, 110(36), 2013.

[21] Beyza Ermis and A Taylan Cemgil. A Bayesian tensor factorization model via variational inference for link prediction. *arXiv preprint arXiv:1409.8276*, 2014.

[22] Aaron Schein, Hanna M Wallach, and Mingyuan Zhou. Poisson-gamma dynamical systems. In *Advances in Neural Information Processing Systems*, 2016.

[23] Lin Yuan and John D Kalbfleisch. On the Bessel distribution and related problems. *Annals of the Institute of Statistical Mathematics*, 52(3), 2000.

[24] Richard A Harshman. Foundations of the PARAFAC procedure: Models and conditions for an "explanatory" multimodal factor analysis. *UCLA Working Papers in Phonetics*, 16, 1970.

[25] Roman N Makarov and Devin Glew. Exact simulation of Bessel diffusions. *Monte Carlo Methods and Applications*, 16(3-4), 2010.

[26] Milton Abramowitz and Irene A Stegun. *Handbook of mathematical functions: with formulas, graphs, and mathematical tables*. Courier Corporation, 1965.

[27] Mingyuan Zhou, Yulai Cong, and Bo Chen. Augmentable gamma belief networks. *Journal of Machine Learning Research*, 17(1), 2016.

[28] Chengyue Gong and Win-bin Huang. Deep dynamic Poisson factorization model. In *Advances in Neural Information Processing Systems*, 2017.

[29] Dandan Guo, Bo Chen, Hao Zhang, and Mingyuan Zhou. Deep Poisson gamma dynamical systems. In *Advances in Neural Information Processing Systems*, 2018.

[30] Ayan Acharya, Joydeep Ghosh, and Mingyuan Zhou. Nonparametric Bayesian factor analysis for dynamic count matrices. In *International Conference on Artificial Intelligence and Statistics*, 2015.

[31] Sikun Yang and Heinz Koeppl. Dependent relational gamma process models for longitudinal networks. In *International Conference on Machine Learning*, 2018.

[32] Mingyuan Zhou and Lawrence Carin. Augment-and-conquer negative binomial processes. In *Advances in Neural Information Processing Systems*, 2012.

[33] Mingyuan Zhou, Yulai Cong, and Bo Chen. The Poisson gamma belief network. In *Advances in Neural Information Processing Systems*, 2015.

[34] A Taylan Cemgil and Onur Dikmen. Conjugate gamma Markov random fields for modelling nonstationary sources. In *International Conference on Independent Component Analysis and Signal Separation*, 2007.

[35] Cédric Févotte, Jonathan Le Roux, and John R Hershey. Non-negative dynamical system with application to speech and audio. In *IEEE International Conference on Acoustics, Speech and Signal Processing*, 2013.

[36] Ghassen Jerfel, Mehmet Basbug, and Barbara Engelhardt. Dynamic collaborative filtering with compound poisson factorization. In *International Conference on Artificial Intelligence and Statistics*, 2017.

[37] Rajesh Ranganath, Linpeng Tang, Laurent Charlin, and David M Blei. Deep exponential families. In *International Conference on Artificial Intelligence and Statistics*, 2015.

[38] Aaron Schein. *Allocative Poisson Factorization for Computational Social Science*. PhD thesis, University of Massachusetts Amherst, 2019.

[39] Robert GD Steel. Relation between Poisson and multinomial distributions. 1953.

[40] Anirban Bhattacharya and David B Dunson. Simplex factor models for multivariate unordered categorical data. *Journal of the American Statistical Association*, 107(497), 2012.

[41] Anne C Smith and Emery N Brown. Estimating a state-space model from point process observations. *Neural Computation*, 15(5), 2003.

[42] Liam Paninski, Yashar Ahmadian, Daniel Gil Ferreira, Shinsuke Koyama, Kamiar Rahnama Rad, Michael Vidne, Joshua Vogelstein, and Wei Wu. A new look at state-space models for neural data. *Journal of Computational Neuroscience*, 29(1-2), 2010.

[43] Jakob H Macke, Lars Buesing, John P Cunningham, Byron M Yu, Krishna V Shenoy, and Maneesh Sahani. Empirical models of spiking in neural populations. In *Advances in Neural Information Processing Systems*, 2011.

[44] Rudolph E Kalman and Richard S Bucy. New results in linear filtering and prediction theory. *Journal of Basic Engineering*, 83(1), 1961.

[45] Zoubin Ghahramani and Sam T Roweis. Learning nonlinear dynamical systems using an EM algorithm. In *Advances in Neural Information Processing Systems*, 1999.

[46] John A Nelder and Robert WM Wedderburn. Generalized linear models. *Journal of the Royal Statistical Society: Series A (General)*, 135(3), 1972.

[47] Laurent Charlin, Rajesh Ranganath, James McInerney, and David M Blei. Dynamic Poisson factorization. In *ACM Conference on Recommender Systems*, 2015.

[48] Patrick T Brandt and Todd Sandler. A Bayesian Poisson vector autoregression model. *Political Analysis*, 20(3), 2012.

[49] Alan G Hawkes. Spectra of some self-exciting and mutually exciting point processes. *Biometrika*, 58(1), 1971.

[50] Aleksandr Simma and Michael I Jordan. Modeling events with cascades of poisson processes. In *Conference on Uncertainty in Artificial Intelligence*, 2010.

[51] Charles Blundell, Jeff Beck, and Katherine A Heller. Modelling reciprocating relationships with Hawkes processes. In *Advances in Neural Information Processing Systems*, 2012.

[52] Scott W Linderman and Ryan Adams. Discovering latent network structure in point process data. In *International Conference on Machine Learning*, 2014.

[53] Luc Devroye. Simulating Bessel random variables. *Statistics & Probability Letters*, 57(3), 2002.

[54] Hanna M Wallach. *Structured topic models for language*. PhD thesis, University of Cambridge Cambridge, UK, 2008.

[55] Hanna M Wallach, Iain Murray, Ruslan Salakhutdinov, and David Mimno. Evaluation methods for topic models. In *International Conference on Machine Learning*, 2009.

[56] Andrew Gelman, Jessica Hwang, and Aki Vehtari. Understanding predictive information criteria for bayesian models. *Statistics and Computing*, 24(6), 2014.

[57] NeurIPS corpus. UCI Machine Learning Repository.

[58] dblp computer science bibliography. http://dblp.uni-trier.de/.

[59] State of the Union Addresses (1790-2006) by United States Presidents. https://www.gutenberg.org/ebooks/5050?msg=welcome_stranger.

[60] Kalev Leetaru and Philip A Schrodt. GDELT: Global data on events, location, and tone, 1979–2012. In *ISA Annual Convention*, volume 2. Citeseer, 2013.

[61] Elizabeth Boschee, Jennifer Lautenschlager, Sean O'Brien, Steve Shellman, James Starz, and Michael Ward. ICEWS coded event data. Harvard Dataverse, 2015.

[62] Saurabh Vyas, Nir Even-Chen, Sergey D Stavisky, Stephen I Ryu, Paul Nuyujukian, and Krishna V Shenoy. Neural population dynamics underlying motor learning transfer. *Neuron*, 97 (5), 2018.

[63] Alex H Williams, Tony Hyun Kim, Forea Wang, Saurabh Vyas, Stephen I Ryu, Krishna V Shenoy, Mark Schnitzer, Tamara G Kolda, and Surya Ganguli. Unsupervised discovery of demixed, low-dimensional neural dynamics across multiple timescales through tensor component analysis. *Neuron*, 98(6), 2018.

[64] Harold W Kuhn. The Hungarian method for the assignment problem. *Naval Research Logistics Quarterly*, 2(1-2), 1955.

Appendix for Poisson-Randomized Gamma Dynamical Systems

Aaron Schein
Data Science Institute
Columbia University

Scott W. Linderman
Department of Statistics
Stanford University

Mingyuan Zhou
McCombs School of Business
University of Texas at Austin

David M. Blei
Department of Statistics
Columbia University

Hanna Wallach
Microsoft Research
New York, NY

1 Shifted confluent hypergeometric (SCH) distribution

The SCH distribution arises in the context of Poisson–gamma–Poisson chains. Consider the following generative process for count m involving latent variables θ and h and fixed $c_1, c_2, c_3, \epsilon_0^{(\theta)} > 0$:

$$m \sim \text{Pois}\left(\theta c_3\right), \tag{1}$$

$$\theta \sim \text{Gam}\left(\epsilon_0^{(\theta)} + h, c_2\right), \tag{2}$$

$$h \sim \text{Pois}\left(c_1\right). \tag{3}$$

As stated in the main paper, when $\epsilon_0 = 0$, a Gibbs sampler based on sampling h and θ from their complete conditionals violates detailed balance since $h \overset{\text{a.s.}}{=} 0$ if $\theta = 0$, and vice versa. Instead, we should sample h from its *incomplete* conditional—i.e., its distribution conditioned on all variables in its Markov blanket except θ:

$$P(h \mid \epsilon_0^{(\theta)} = 0, -\backslash\theta) \triangleq \int P(h, \theta \mid \epsilon_0^{(\theta)} = 0, -)\, \mathbf{d}\theta. \tag{4}$$

Integrating θ out of the generative process given in Equations (1) to (3) yields the following generative process for m as a negative binomial random variable, where $p \triangleq \frac{c_3}{c_3 + c_2}$:

$$m \sim \text{NB}\left(h,\, p\right), \tag{5}$$

$$h \sim \text{Pois}\left(c_1\right). \tag{6}$$

By Bayes' rule, the posterior of h given m is equal to:

$$P(h \mid m, c_1, p) = \frac{\text{Pois}\left(h; c_1\right) \text{NB}\left(m; h, p\right)}{P(m \mid c_1, p)}. \tag{7}$$

To find a closed form for this expression we need a closed form for the denominator. When the negative binomial has a count-valued first parameter, it is referred to as the *Pascal distribution* [1]. The construction in Equations (5) to (6) describes a Pascal variable with a Poisson-distributed first parameter—the marginal distribution of m with h marginalized out has been called the *Poisson–Pascal distribution* [2], which is a special case of the *Polya–Aeppli distribution* [1]:

$$P(m \mid c_1, p) = \sum_{h=0}^{\infty} \text{Pois}\left(h; c_1\right) \text{NB}\left(m; h, p\right) \tag{8}$$

$$= \text{Polya-Aeppli}\left(m;\, c_1, p\right). \tag{9}$$

The Polya-Aeppli distribution is defined by two parameters—$p \in (0,1)$ and $c \geq 0$—and PMF:

$$\text{Polya-Aeppli}\,(m;\, c, p) = \begin{cases} e^{-p\,c} & \text{if } m = 0 \\ e^{-c_1} c\, p^m (1-p)\, {}_1\text{F}_1\big(m+1; 2; c(1-p)\big) & \text{otherwise,} \end{cases} \tag{10}$$

where ${}_1\text{F}_1\big(a; b; z\big)$ is Kummer's confluent hypergeometric function [3].

Plugging in the Polya-Aeppli PMF into the denominator of Eq. (7) (and the Poisson and negative binomial PMFs into the numerator) we obtain a closed-form expression for the posterior of h. Since the Polya-Aeppli's PMF is different for $m=0$ and $m > 0$, we first consider the case where $m=0$:

$$P(h \,|\, m=0, c_1, p) = \frac{\text{Pois}\,(h; c_1)\,\text{NB}\,(0; h, p)}{\text{Polya-Aeppli}(0; c_1, p)} \tag{11}$$

$$= \frac{\frac{(c_1)^h}{h!} e^{-c_1} (1-p)^h}{e^{-p\,c_1}} \tag{12}$$

$$= \frac{[c_1(1-p)]^h}{h!} e^{-c_1(1-p)}. \tag{13}$$

We recognize this as the form of a Poisson PMF with parameter $\zeta \triangleq c_1(1-p)$:

$$= \text{Pois}\,(h; \zeta). \tag{14}$$

Thus, when $m=0$, the posterior of h is Poisson. The posterior of h when $m > 0$ is:

$$P(h \,|\, m>0, c_1, p) = \frac{\text{Pois}\,(h; c_1)\,\text{NB}\,(m; h, p)}{\text{Polya-Aeppli}(m; c_1, p)} \tag{15}$$

$$= \frac{\frac{(c_1)^h}{h!} e^{-c_1} \frac{\Gamma(m+h)}{m!\,\Gamma(h)} p^m (1-p)^h}{e^{-c_1} c_1\, p^m (1-p)\, {}_1\text{F}_1\big(m+1; 2; c_1(1-p)\big)} \tag{16}$$

$$= \frac{\frac{\Gamma(m+h)}{h!\,m!\,\Gamma(h)} [c_1(1-p)]^{h-1}}{{}_1\text{F}_1\big(m+1; 2; c_1(1-p)\big)}. \tag{17}$$

Since c_1 and h always appear together, we plug in ζ as defined in Eq. (14), to obtain

$$= \frac{\frac{\Gamma(m+h)}{h!\,m!\,\Gamma(h)}\, \zeta^{h-1}}{{}_1\text{F}_1\big(m+1; 2; \zeta\big)}, \tag{18}$$

which is a discrete distribution defined by two parameters—$\zeta > 0$ and $m \in \{1, 2, \dots\}$. When $m > 0$, $h \overset{\text{a.s.}}{>} 0$ since $m \overset{\text{a.s.}}{=} 0$ if $h=0$. Thus, this distribution is defined on the support $h \in \{1, 2, \dots\}$.

What is this distribution? It is illustrative to consider its probability generating function (PGF):

$$G(s) = \mathbb{E}\big[s^h \,|\, m, \zeta\big] \tag{19}$$

$$= \sum_{h=1}^{\infty} s^h \frac{\frac{\Gamma(m+h)}{h!\,m!\,\Gamma(h)}\, \zeta^{h-1}}{{}_1\text{F}_1\big(m+1; 2; \zeta\big)} \tag{20}$$

$$= s\, \frac{{}_1\text{F}_1\big(m+1; 2; s\zeta\big)}{{}_1\text{F}_1\big(m+1; 2; \zeta\big)}. \tag{21}$$

The PGF in Eq. (21) nearly matches that of the *confluent hypergeometric distribution* [1]. The confluent hypergeometric distribution $h \sim \text{ConfHyp}(h; a, b, z)$ is a discrete distribution over counts $h \in \{0, 1, 2, \dots\}$ defined by three parameters $a, b, z > 0$ and PGF equal to $G'(s) = \frac{{}_1\text{F}_1(a;b;sz)}{{}_1\text{F}_1(a;b;z)}$. The s out in front of the PGF in Eq. (21) is the only difference between it and the PGF of a confluent hypergeometric distribution with parameters $a=m+1$, $b=2$, and $z = \zeta$. However, the following

2

manipulation reveals that the PGF in Eq. (21) defines a *shifted* confluent hypergeometric distribution:

$$G(s) = sG'(s) \tag{22}$$

$$= s \sum_{h=0}^{\infty} s^h \, \text{ConfHyp}(h; m+1, 2, \zeta) \tag{23}$$

$$= \sum_{h=1}^{\infty} s^h \, \text{ConfHyp}(h-1; m+1, 2, \zeta). \tag{24}$$

The posterior distribution of h when $m > 0$ can thus appropriately be described as a *shifted confluent hypergeometric (SCH) distribution*. An SCH random variable $h \sim \text{SCH}(m, \zeta)$ can be generated as $h \triangleq n+1$ where $n \sim \text{ConfHyp}(m+1, 2, \zeta)$.

1.1 Proof of Theorem 1

Theorem 1: *The incomplete conditional* $P(h \,|\, \epsilon_0^{(\theta)} = 0, -\backslash\theta) \triangleq \int P(h, \theta \,|\, \epsilon_0^{(\theta)} = 0, -) \, \mathrm{d}\theta$ *is*

$$(h \,|\, -\backslash\theta) \sim \begin{cases} \text{Pois}\left(\frac{c_1 c_2}{c_3 + c_2}\right) & \text{if } m = 0 \\ \text{SCH}\left(m, \frac{c_1 c_2}{c_3 + c_2}\right) & \text{otherwise.} \end{cases} \tag{25}$$

Proof: The preceding derivation constitutes the proof—in particular, see Eq. (14) and Eq. (18).

1.2 Sampling from the SCH distribution

As stated above, an SCH random variable can be generated in terms of a confluent hypergeometric random variable. However, we are unaware of any open-source implementation for sampling from the confluent hypergeometric distribution.

We implement a table sampler for the SCH distribution by directly evaluating its PMF at candidate values. This sampler is efficient if we begin with mode h^* as the first candidate value and then step out h^*-1 or h^*+1 (if the mode is not accepted). Since the confluent hypergeometric distribution is unimodal and underdispersed [1], the SCH is as well—thus, a table sampler that begins at the mode frequently terminates after a small number iterations, since the PMF quickly and monotonically decays in both directions from the mode.

To derive the mode of the SCH, we appeal to the fact that any PMF has the following property,

$$P(H = h^*-1) \le P(H = h^*) \ge P(H = h^*+1), \tag{26}$$

which can be equivalently stated in terms of the following two equations:

$$\frac{P(H = h^*)}{P(H = h^*-1)} \ge 1, \tag{27}$$

$$\frac{P(H = h^*)}{P(H = h^*+1)} \le 1. \tag{28}$$

Plugging in the PMF of the SCH distribution we obtain the following two inequalities:

$$\frac{\zeta(h^* + m - 1)}{h^*(h^* - 1)} \ge 1, \tag{29}$$

$$\frac{\zeta(h^* + m)}{h^*(h^* + 1)} \le 1. \tag{30}$$

Solving this system of inequalities gives us the following bounds on h^*:

$$f(\zeta, m) - 0.5 \le h^* \le f(\zeta, m) + 0.5, \tag{31}$$

where $f(\zeta, m) \triangleq \frac{1}{2}\left(\sqrt{2\zeta(2m-1) + \zeta^2 + 1} + \zeta\right)$. Since h discrete, the mode of the SCH is

$$\text{mode}\,(h; m, \zeta) = \left\lfloor \frac{1}{2}\left(\sqrt{2\zeta(2m-1) + \zeta^2 + 1} + \zeta\right) \right\rfloor, \tag{32}$$

which does involve any special functions and is thus efficient to compute.

3

2 Closed-form complete conditionals for the PRGDS

Recall that the per-component weights λ_k appear in the Poisson rate of each observed count $y_{\mathbf{i}}^{(t)} \sim \text{Pois}\left(\rho^{(t)} \sum_{k=1}^{K} \lambda_k \theta_k^{(t)} \prod_{m=1}^{M} \phi_{ki_m}^{(m)}\right)$ as well as in the Poisson rate of the first latent discrete state $h_{k\cdot}^{(1)} \sim \text{Pois}\left(\tau \sum_{k_2=1}^{K} \pi_{kk_2}\lambda_{k_2}\right)$. Consider the following sum of latent sources $y_{\cdot k}^{(\cdot)} \triangleq \sum_{t=1}^{T} \sum_{\mathbf{i}} y_{\mathbf{i}k}^{(t)}$—it is a Poisson random variable $y_{\cdot k}^{(\cdot)} \sim \text{Pois}\left(\lambda_k \omega_k\right)$ where $\omega_k \triangleq \prod_{m=1}^{M} \phi_{k\cdot}^{(m)} \sum_{t=1}^{T} \rho^{(t)}\theta_k^{(t)}$. Now define $h_{\cdot k}^{(1)} \triangleq \sum_{k_1=1}^{K} h_{k_1 k}^{(1)}$ to be the sum of the kth column of the first ($t=1$) matrix of latent counts—it is distributed $h_{\cdot k}^{(1)} \sim \text{Pois}\left(\lambda_k \tau \pi_{\cdot k}\right)$. Finally, define the sum $m_k^{(\lambda)} \triangleq h_{\cdot k}^{(1)} + y_{\cdot k}^{(\cdot)}$ which isolates all dependence on λ_k and is Poisson $m_k^{(\lambda)} \sim \text{Pois}\left(\lambda_k(\tau\pi_{\cdot k} + \omega_k)\right)$. By gamma–Poisson conjugacy, the complete conditional for λ_k is thus

$$\left(\lambda_k \mid -\right) \sim \text{Gam}\left(\epsilon_0^{(\lambda)} + g_k + m_k^{(\lambda)},\ \beta + \tau\pi_{\cdot k} + \omega_k\right), \tag{33}$$

$$m_k^{(\lambda)} \triangleq \left(\sum_{t=1}^{T} \sum_{\mathbf{i}} y_{\mathbf{i}k}^{(t)}\right) + \left(\sum_{k_1=1}^{K} h_{k_1 k}^{(1)}\right), \tag{34}$$

$$\omega_k \triangleq \prod_{m=1}^{M} \phi_{k\cdot}^{(m)} \sum_{t=1}^{T} \rho^{(t)}\theta_k^{(t)}. \tag{35}$$

We may apply the identifies on Poisson–gamma–Poisson chains provided in the main paper to derive the complete conditional for g_k when $\epsilon_0^{(\lambda)} > 0$ as

$$\left(g_k \mid -\right) \sim \text{Bessel}\left(\epsilon_0^{(\lambda)} - 1,\ 2\sqrt{\lambda_k \beta \tfrac{\gamma}{K}}\right), \tag{36}$$

and for $\epsilon_0^{(\lambda)} = 0$ as

$$\left(g_k \mid -\right) \sim \text{SCH} \begin{cases} \text{Pois}\left(\zeta_k^{(\lambda)}\right) & \text{if } m_k^{(\lambda)} = 0 \\ \text{SCH}\left(m_k^{(\lambda)}, \zeta_k^{(\lambda)}\right) & \text{otherwise,} \end{cases} \tag{37}$$

$$\zeta_k^{(\lambda)} \triangleq \frac{\beta \tfrac{\gamma}{K}}{\tau\pi_{\cdot k} + \omega_k + \beta}. \tag{38}$$

By gamma–Poisson and gamma–gamma conjugacy the complete conditionals for γ and β are

$$\left(\gamma \mid -\right) \sim \text{Gam}\left(a_0 + g_\cdot,\ b_0 + 1\right), \tag{39}$$

$$\left(\beta \mid -\right) \sim \text{Gam}\left(\alpha_0 + K\epsilon_0^{(\lambda)} + g_\cdot,\ \alpha_0 + \lambda_\cdot\right). \tag{40}$$

By both gamma–gamma and gamma–Poisson conjugacy, the complete conditional for τ is gamma:

$$\left(\tau \mid -\right) \sim \text{Gam}\left(\alpha_0 + TK\epsilon_0^{(\theta)} + 2\,h_{\cdot\cdot}^{(\cdot)},\ \alpha_0 + \lambda_\cdot + \theta_\cdot^{(\cdot)} + \sum_{k=1}^{K}\sum_{t=2}^{T-1}\sum_{k_2=1}^{K} \pi_{kk_2}\theta_{k_2}^{(t-1)}\right). \tag{41}$$

By Dirichlet–multinomial conjugacy, the complete conditional for $\boldsymbol{\pi}_k$ is Dirichlet:

$$\left(\boldsymbol{\pi}_k \mid -\right) \sim \text{Dir}\left(a_0 + h_{1k}^{(\cdot)}, \ldots, a_0 + h_{Kk}^{(\cdot)}\right). \tag{42}$$

By Dirichlet–multinomial conjugacy, the complete conditional for each factor vector $\boldsymbol{\phi}_k^{(m)}$ is

$$\left(\boldsymbol{\phi}_k^{(m)} \mid -\right) \sim \text{Dir}\left(a_0 + \sum_{\mathbf{i}:\mathbf{i}_m=1} y_{\mathbf{i}k}^{(t)}, \cdots, a_0 + \sum_{\mathbf{i}:\mathbf{i}_m=L_m} y_{\mathbf{i}k}^{(t)}\right), \tag{43}$$

where the sum $\sum_{\mathbf{i}:\mathbf{i}_m=d}$ sums over all values of the multi-index $\mathbf{i} = (\mathbf{i}_1, \ldots, \mathbf{i}_M)$ that have the mth index equal to a specific value $\mathbf{i}_m = d$.

By gamma–Poisson conjugacy, the complete conditional for $\rho^{(t)}$ or ρ (for the stationary variant) are

$$\left(\rho^{(t)} \mid -\right) \sim \text{Gam}\left(a_0 + y_\cdot^{(t)},\ b_0 + \omega^{(t)}\right), \tag{44}$$

$$\left(\rho \mid -\right) \sim \text{Gam}\left(a_0 + y_\cdot^{(\cdot)},\ b_0 + \sum_{t=1}^{T} \omega^{(t)}\right), \tag{45}$$

where $\omega^{(t)} \triangleq \sum_{k=1}^{K} \lambda_k \prod_{m=1}^{M} \phi_{k\cdot}^{(m)}\theta_k^{(\cdot)}$.

3 Tensor generalization of the PGDS

3.1 Original generative process

Schein et al. (2016) [4] originally introduced the PGDS to model $T \times V$ count matrices Y—the PGDS assumes each count $y_v^{(t)}$ in the matrix is a Poisson random variable:

$$y_v^{(t)} \sim \text{Pois}\Big(\rho^{(t)} \sum_{k=1}^{K} \theta_k^{(t)} \phi_{kv}\Big). \tag{46}$$

The states $\theta_k^{(t)}$ evolve as

$$\theta_k^{(t)} \sim \text{Gam}\left(\tau \sum_{k_2=1}^{K} \pi_{kk_2}\theta_{k_2}^{(t-1)}, \tau\right). \tag{47}$$

The columns of the factor matrix Φ are Dirichlet distributed:

$$\phi_k \sim \text{Dir}(a_0, \ldots a_0). \tag{48}$$

See the original paper [4] for more details.

3.2 Generative process for tensor generalization

The PGDS can be generalized to be a canonical polyadic (CP) decomposition [5] of sequentially observed M-mode tensors by assuming each count $y_{\mathbf{i}}^{(t)}$ is

$$y_{\mathbf{i}}^{(t)} \sim \text{Pois}\Big(\rho^{(t)} \sum_{k=1}^{K} \theta_k^{(t)} \prod_{m=1}^{M} \phi_{k\mathbf{i}_m}^{(m)}\Big). \tag{49}$$

The states $\theta_k^{(t)}$ evolve the same as in Eq. (47). There are now M different factor matrices—the columns of the mth matrix $\Phi^{(m)}$ are Dirichlet distributed:

$$\phi_k^{(m)} \sim \text{Dir}(a_0, \ldots a_0). \tag{50}$$

All other aspects are the same as the matrix version.

3.3 Complete conditionals

The latent sources for the tensor PGDS have the following complete conditional:

$$\big((y_{\mathbf{i}k}^{(t)})_{k=1}^{K} \,|\, - \big) \sim \text{Multinom}\left(y_{\mathbf{i}}^{(t)}, \big(\theta_k^{(t)} \prod_{m=1}^{M} \phi_{k\mathbf{i}_m}^{(m)}\big)_{k=1}^{K}\right). \tag{51}$$

By Dirichlet–multinomial conjugacy, each column of the mth has the following complete conditional:

$$\big(\phi_k^{(m)} \,|\, - \big) \sim \text{Dir}\left(a_0 + \sum_{\mathbf{i}:\mathbf{i}_m=1} y_{\mathbf{i}k}^{(t)}, \cdots, a_0 + \sum_{\mathbf{i}:\mathbf{i}_m=L_m} y_{\mathbf{i}k}^{(t)}\right), \tag{52}$$

where the sum $\sum_{\mathbf{i}:\mathbf{i}_m=d}$ sums over all values of the multi-index $\mathbf{i} = (\mathbf{i}_1, \ldots, \mathbf{i}_M)$ that have the mth index equal to a specific value $\mathbf{i}_m = d$.

All other complete conditionals are the same as in matrix version (see the original paper).

5

# 4 Qualitative analysis of latent structure inferred from ICEWS data

We qualitatively compared the latent structure inferred by the two PRGDS variants and the PGDS on ICEWS international events data. To do so, we aligned the inferred components of one model to another using the Hungarian bipartite matching algorithm [6] applied to their inferred $K \times T$ gamma state matrices. The kth component's activation vector $\boldsymbol{\theta}_k = (\theta_k^{(1)}, \ldots, \theta_k^{(T)})$ constitutes a signature of that component's activity; these signatures are sufficiently unique to facilitate alignment.

We interpret the components as *multilateral relations* [7], where a component is characterized by its activation vector $\boldsymbol{\theta}_k$ (i.e., when that component is active), who the typical sender $\phi_k^{(1)}$ and receiver $\phi_k^{(2)}$ countries are, and what action types $\phi_k^{(3)}$ are typically used. We found the vast majority of inferred components to be well aligned across all three models. In Figures 1 to 4, we provide four examples of components inferred by each of the three models that were aligned to each other by the matching algorithm. We visualize each component's $\boldsymbol{\theta}_k$ in chronological order in the top panel of each plot. The bottom-left stem plot displays the top values of sender parameters, in descending order. If fewer than ten senders account for more than 99% of the mass, we only display their names; otherwise, the top seven are given. The same is true for the bottom-middle and bottom-right stem plots, corresponding to receivers and action types. We see that all four aligned components measure a qualitatively similar multilateral relation corresponding respectively to the Israeli–Palestinian conflict (Fig. 1), Vietnamese international relations (Fig. 2), Central European relations (Fig. 3), and West African relations (Fig. 4).

There were only a few instances where the aligned components were qualitatively dissimilar. In particular, we found a few cases where the aligned components of the PGDS and the non-sparse variant of the PRGDS were qualitatively similar, but the component inferred by the sparse variant of the PRGDS had no counterpart. This occurred when the component inferred by the sparse variant featured a highly localized pattern. The component visualized in the main text is such an example.

References

[1] Norman L Johnson, Adrienne W Kemp, and Samuel Kotz. *Univariate discrete distributions*. John Wiley & Sons, 2005.

[2] SK Katti and John Gurland. The Poisson Pascal distribution. *Biometrics*, 17(4), 1961.

[3] Milton Abramowitz and Irene A Stegun. *Handbook of mathematical functions: with formulas, graphs, and mathematical tables*. Courier Corporation, 1965.

[4] Aaron Schein, Hanna M Wallach, and Mingyuan Zhou. Poisson-gamma dynamical systems. In *Advances in Neural Information Processing Systems*, 2016.

[5] Richard A Harshman. Foundations of the PARAFAC procedure: Models and conditions for an "explanatory" multimodal factor analysis. *UCLA Working Papers in Phonetics*, 16, 1970.

[6] Harold W Kuhn. The Hungarian method for the assignment problem. *Naval Research Logistics Quarterly*, 2(1-2), 1955.

[7] Aaron Schein, John Paisley, David M Blei, and Hanna M Wallach. Bayesian Poisson tensor factorization for inferring multilateral relations from sparse dyadic event counts. In *ACM SIGKDD International Conference on Knowledge Discovery and Data Mining*, 2015.
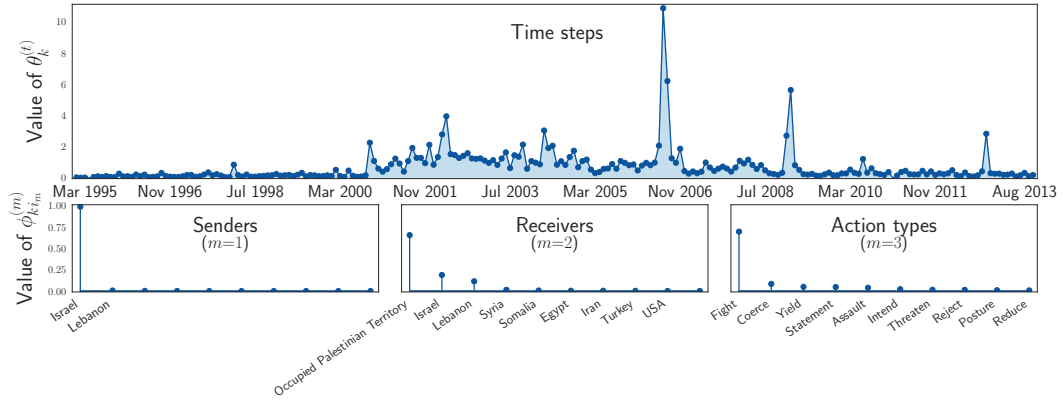
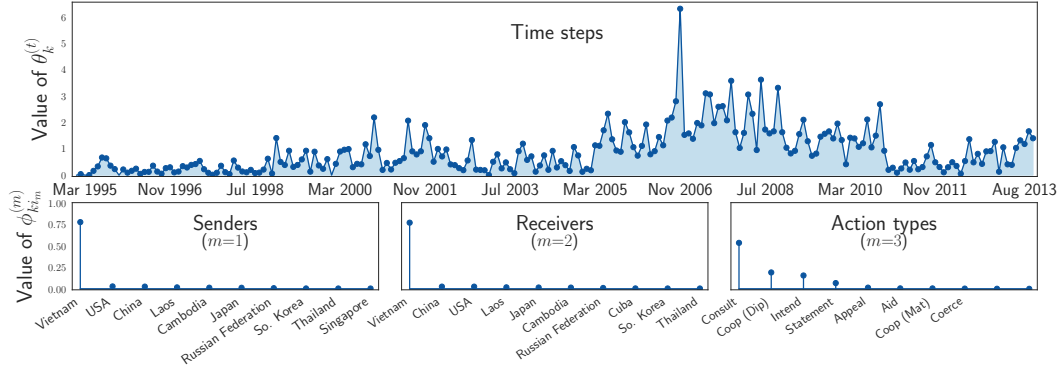(a) Component inferred by the sparse PRGDS ($\epsilon_0^{(\theta)} = 0$).
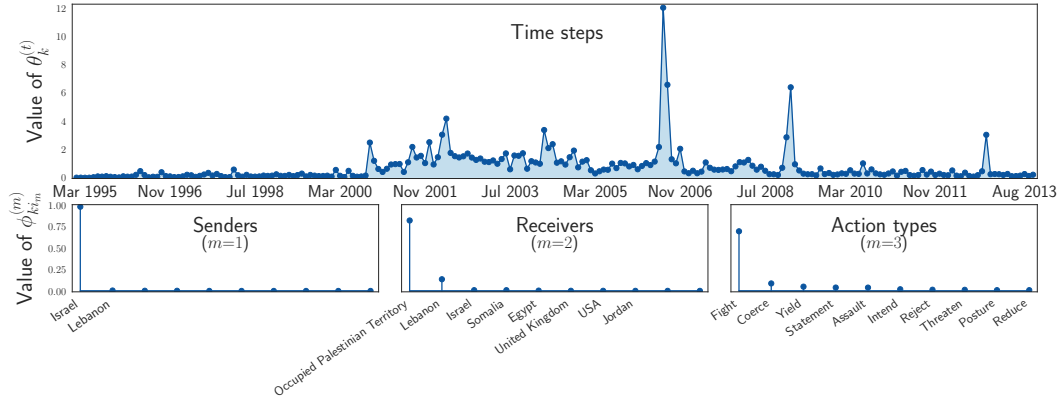
(b) Component inferred by the non-sparse PRGDS ($\epsilon_0^{(\theta)} = 1$).
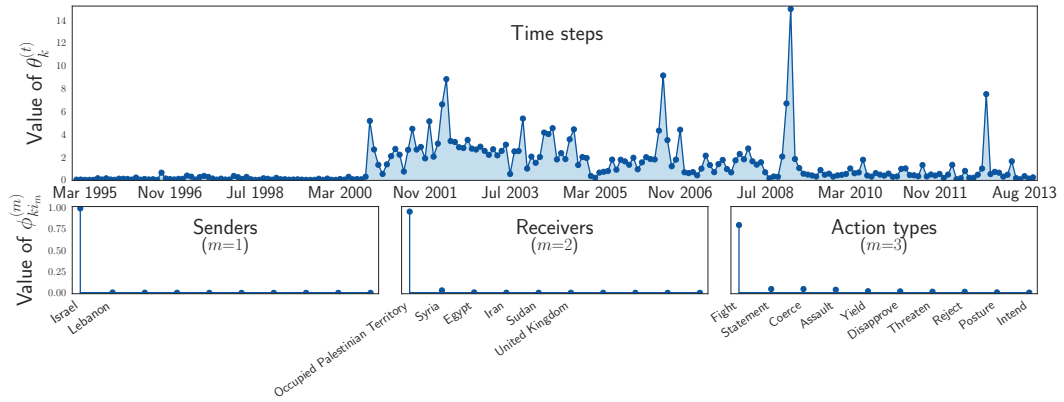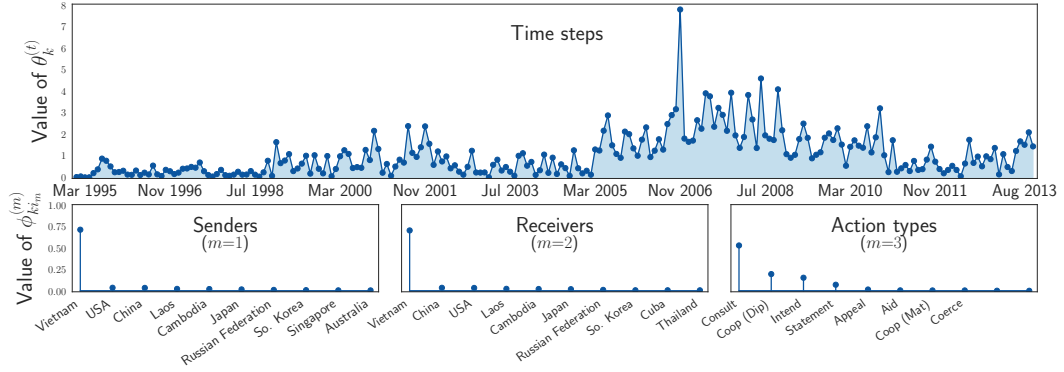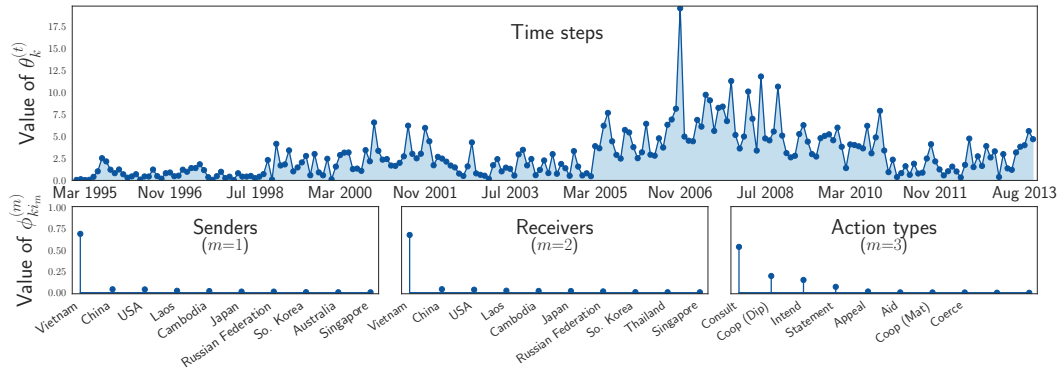

(c) Component inferred by the PGDS.

Figure 1: A component aligned across all three models that measures the Israeli–Palestinian conflict.

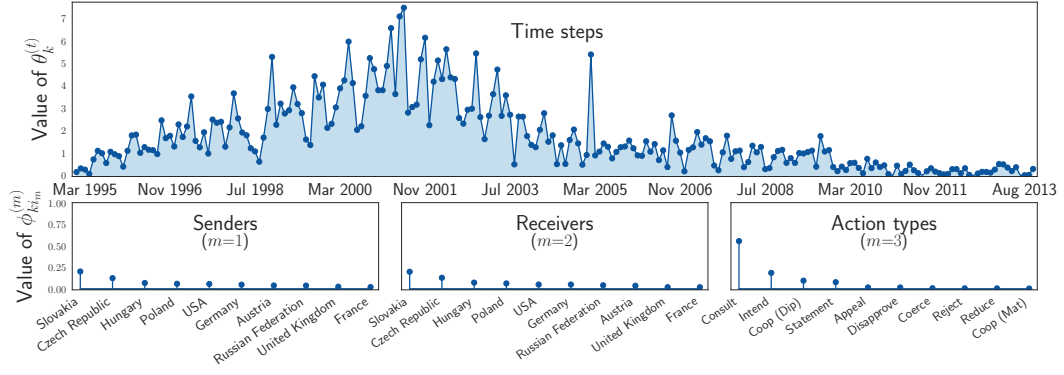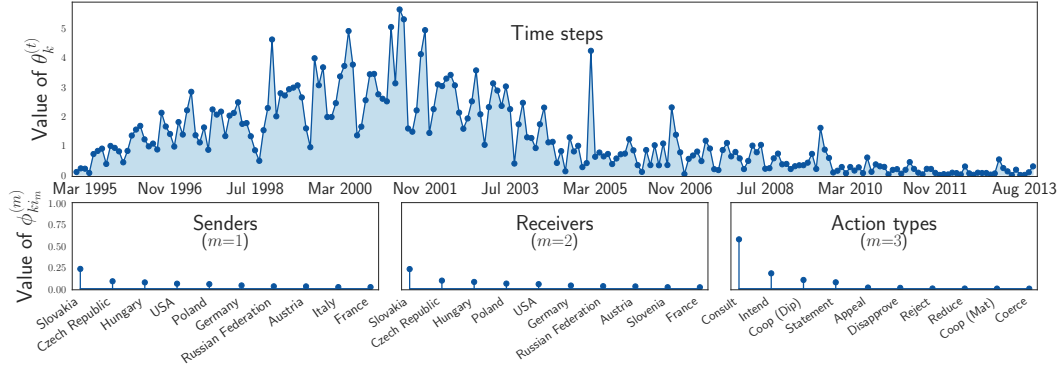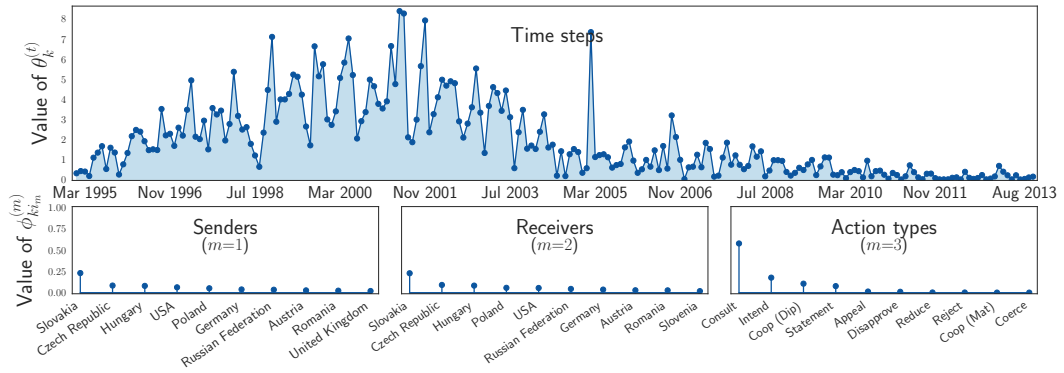(a) Component inferred by the sparse PRGDS ($\epsilon_0^{(\theta)} = 0$).

(b) Component inferred by the non-sparse PRGDS ($\epsilon_0^{(\theta)} = 1$).

(c) Component inferred by the PGDS.

Figure 2: A component aligned across all three models that measures Vietnamese relations.

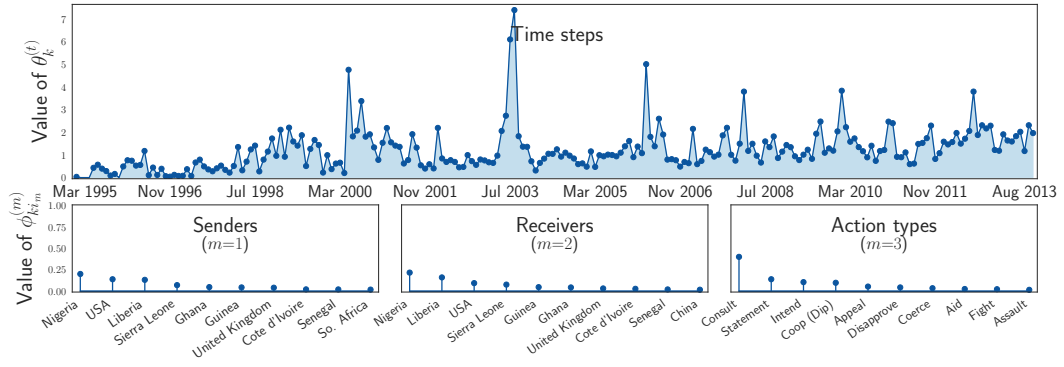(a) Component inferred by the sparse PRGDS ($\epsilon_0^{(\theta)} = 0$).

(b) Component inferred by the non-sparse PRGDS ($\epsilon_0^{(\theta)} = 1$).
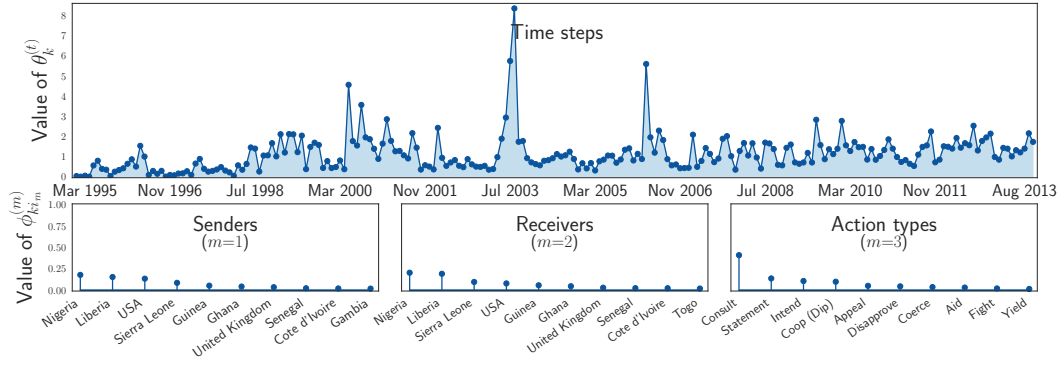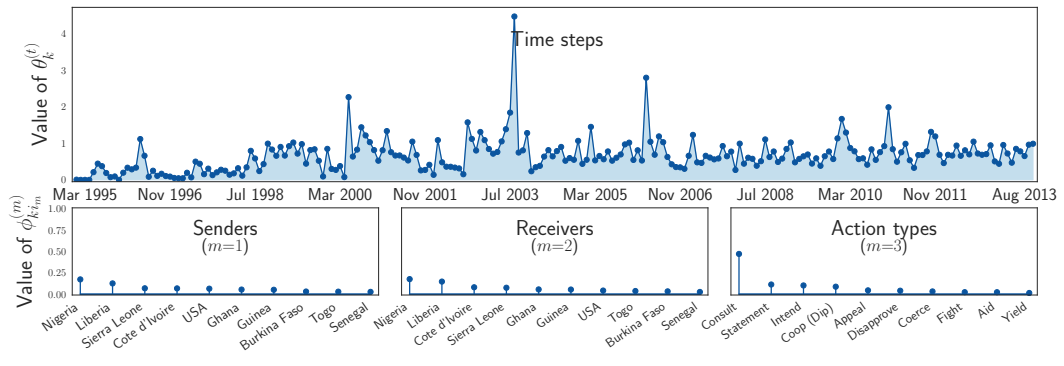

(c) Component inferred by the PGDS.

Figure 3: A component aligned across all three models that measures Central European relations.

(a) Component inferred by the sparse PRGDS ($\epsilon_0^{(\theta)} = 0$).

(b) Component inferred by the non-sparse PRGDS ($\epsilon_0^{(\theta)} = 1$).

(c) Component inferred by the PGDS.

Figure 4: A component aligned across all three models that measures West African relations.